Full Paper

Ionic Liquid-based Microchannels for Highly Sensitive and Fast Amperometric Detection of Toxic Gases

Mengchen Ge [a] *†, Ghulam Hussain* [b] *†, D. Brynn Hibbert* [a]*, Debbie S. Silvester* [b] *, and Chuan Zhao* [a] *

[a] School of Chemistry, Faculty of Science, The University of New South Wales, Sydney 2052, Australia
[b] Curtin Institute for Functional Molecules and Interfaces, School of Molecular and Life Sciences, Curtin University, GPO Box U1987, Perth, 6845, WA, Australia
† These authors contributed equally to this work.
* Corresponding author e-mail addresses: chuan.zhao@unsw.edu.au, d.silvester-dean@curtin.edu.au

Abstract
Ionic liquid (IL)-based microchannels sensors have been fabricated and employed for the detection of toxic ammonia (NH_3) and hydrogen chloride (HCl) gases, with enhanced sensitivity and response times compared to conventional electrodes. Electrochemical techniques were employed to understand the behaviour of these highly toxic gases in two ionic liquids, [C_4mpyrr][NTf_2] and [C_2mim][NTf_2], on a gold modified microchannels electrode. The limits of detection (LODs) obtained in [C_4mpyrr][NTf_2] for NH_3 (3.7 ppm) and in [C_2mim][NTf_2] for HCl (3.6 ppm) were lower than the current Occupational Safety and Health Administration Permissible Exposure Limit (OSHA PEL) for the two gases (25 ppm for NH_3 and 5 ppm for HCl). The response time of the sensor is 15 s with a sensitivity of 143 nA ppm^{-1} and 14 nA ppm^{-1} for HCl and NH_3, respectively. These results demonstrate the superiority of IL-based microchannels sensors for detecting toxic gases, when compared to commercially available sensors or traditional IL-based sensor designs, where high sensitivity or fast response time is still a challenge.

Keywords: Ionic liquid, ammonia oxidation, proton reduction, linear sweep voltammetry, chronoamprometry

1. Introduction

Gas detection is extremely important to applications in environmental and occupational health and safety (OHS) sectors [1-3]. In particular, it is essential to continuously monitor harmful or toxic gases, such as ammonia (NH_3) and hydrogen chloride (HCl) emissions, which could come from man-made sources [4-6] (e.g. plastic burning, waste disposal sites or industrial processes) and threaten public health [7, 8]. Malek and Alarie reported that guinea pigs exposure to 162 parts per million (ppm) and 586 ppm HCl are incapacitated after an average of 1.3 min and 0.6 min, respectively [9]. All animals in the highest exposure group died within an average of 3 min. As for NH_3, it has been reported that a 5 minute exposure to 72 or 134 ppm will cause nasal, eye, throat irritation and lacrimation for most people [10]. In this case, a rapid response as well as high sensitivity are very important for toxic gas sensors.

Among the wide range of sensors employed to monitor toxic gases, amperometric gas sensors (AGSs) are mostly used due to their low cost, high sensitivity, fast response and small size that enables portability [11]. Conventional AGSs detect the analyte gas by measuring changes in current across a target-specific electrode. A Clark-type AGS usually consists of three electrodes (working, reference and counter), a porous membrane and a solvent as the electrolyte. Analyte gases pass through the porous membrane and diffuse into the electrolyte. When the analyte gas contacts the electrode, an electrochemical reaction takes place, producing a change in current. However, commercially available AGSs are not suitable for use in harsh conditions (for example dry conditions or high temperatures). For example, a commercial HCl AGS (0–100 ppm, HCl-A1 series) from Alphasense is unable to be operated above 50 °C (Manufacturer's datasheets – Alphasense.com). Even under normal atmospheric conditions, the electrolyte is prone to drying due to the volatility of the

solvent (e.g. sulfuric acid), thus giving a shorter lifetime of the sensor. The membrane has been employed to reduce the evaporation rate, but is unable to eliminate the problem completely.

Room temperature ionic liquids (RTILs) possess a series of superior properties, such as low volatility, and they can be seen as suitable replacements for conventional solvents in membrane-free AGSs [12, 13]. The high thermal stability of RTILs allows the sensors to satisfy operating temperature requirements in the real world (e.g. up to 60 °C) which is much higher compared to conventional solvents [14]. In addition, the detection of NH_3 and HCl (two gases that are studied in this work) at very low concentrations will benefit from the high solubility of polar gases in ILs [15-18]. Murugappan *et al.* investigated the mechanism and sensing performance for HCl gas in several RTILs [19]. They reported the limit of detection (LOD) calculated using the currents from the oxidation of $[HCl_2]^-$ and reduction of H^+ with concentrations between 104−2048 ppm is 102 ppm and 69 ppm, respectively. The same group also reported a microarray thin film electrode (MATFE) for detecting NH_3 in $[C_2mim][NTf_2]$ [20]. Excellent stability and reproducibility were observed on the recessed and filled MATFEs. A LOD of 0.02 ppm on the filled MATFE is believed to be the lowest LOD reported for NH_3 in pure RTILs. The above-mentioned works, in addition to various other studies [21-23], have shown that there is a promising prospect as well as driving force towards the combination of RTILs and miniaturization of AGSs for toxic gas detection.

However, RTILs are much more viscous than conventional solvents, resulting in slow diffusion of the analyte gas and thus decreasing the sensitivity and prolonging the response time of the sensor. Carter *et al.* fabricated a series of printed amperometric NH_3 sensors with a low LOD less than 2 ppm but with long response time up to 390 s [23, 24]. Therefore, a RTIL-based AGS with fast response and high sensitivity is still a challenge and is highly desired. Recently, Gunawan *et al.* demonstrated a strategy to fabricate ionic liquid microarrays by utilising microcontact printing for oxygen gas sensing [25]. The small volume (~pL) of IL droplets generated extremely thin layers on the electrode surface. The overall oxygen sensing performance is greatly enhanced by significantly decreasing the diffusion path of oxygen molecules to the electrodes. Compared to a macroscopic electrode sensor, the IL-based microarray sensor has a faster response time (10 seconds faster τ_{90}, 45.2 s vs. 55.6 s) and higher sensitivity to oxygen in the range of 130−1,450 ppm, where the macroscopic electrode sensor fails to respond.

In this work, an IL-based array of microchannels has been fabricated by microcontact printing and utilized, for the first time, for the detection of toxic gases, demonstrating rapid response times, high sensitivity and low LODs. The extremely small volume of RTILs applied in this design aims to reduce the diffusion distance and thus gives a faster response time. Additionally, the high surface to volume ratio of the microarray has been demonstrated to increase the sensitivity of the sensor [26]. Two different hydrophobic RTILs are used for the fabrication of the IL-microchannel array based gas sensor, and two different detection methods – linear sweep voltammetry and chronoamperometry – are studied.

2. Experimental Section

2.1 Chemicals

Ultrapure water was used for preparation of the self-assembled monolayer (SAM) solutions and for rinsing. 1-ethyl-3-methylimidazolium bis(trifluoromethyl-sulfonyl)imide ($[C_2mim][NTf_2]$) (99%) was purchased from Merck, Kilsyth, Victoria, and 1-butyl-1-methylpyrrolidinium bis(trifluoromethylsulfonyl)imide ($[C_4mpyrr][NTf_2]$) (99%) was purchased from IoLiTec Ionic Liquids Technologies GmbH and used without further purification. 1-hexadecanethiol (HDT, 99%) was used as received from Sigma-Aldrich (Sydney, Australia). Nitrogen (N_2) gas (for further dilution of the analyte gas) was obtained from a 99.99% purity N_2 cylinder (BOC gases, Welshpool, WA, Australia). Ammonia and hydrogen chloride gases (500 ppm NH_3, 2000 ppm HCl, nitrogen fill) were purchased from CAC gases (Auburn, NSW, Australia).

2.2 Fabrication of IL-based Microchannels Electrode

Polydimethyl siloxane (PDMS) stamps were prepared from Si/SU8 masters and Sylgard 184 PDMS (Dow Corning Corporation) as per the method outlined by Whitesides *et al.* [27] The SAM solutions prepared by mixing one drop of HDT with 10 mL ethanol, and then sonicated for 3 mins to obtain well-dissolved solutions. The PDMS stamp was inked with the ethanolic HDT solution and printed onto a gold substrate without refilling the gaps. The gold substrate was rinsed twice with ethanol to remove excess HDT and then dried under a gentle nitrogen stream. A drop of IL ($[C_2mim][NTf_2]$ or $[C_4mpyrr][NTf_2]$) was brought into contact with the patterned area on the gold substrate. Excess IL was removed by slow back suction with the micropipette or by blowing with nitrogen gas.

2.3 Electrochemical Experiments

All electrochemical experiments were performed using a PGSTAT101 (Metrohm Autolab, Netherlands) interfaced to a PC with NOVA version 1.11 software. A three-electrode cell (Au macro working electrode with microchannels, Pt wire counter and Ag wire reference electrode) was employed and connected directly to the potentiostat via crocodile clips. The cell was first purged with N_2 gas to remove impurities naturally present in the IL (e.g. oxygen, water). Due to the small volume and high surface area of the RTIL microchannels, the time taken to stabilize was relatively short (~20 mins). When the baseline was stable, the toxic gas analyte – NH_3 or HCl – was introduced into one arm of the cell. The gas was allowed to partition into the RTIL until equilibrium was obtained. An outlet gas line (PTFE tube) led from the other arm of the cell into a fume cupboard. All experiments were carried out at laboratory temperature of (295 ± 2) K.

2.4 Physical Characterizations

All reflection microscopy images were recorded using a Nikon Eclipse TS100-F inverted microscope (Nikon, Japan) and a Nikon Eclipse LV150L microscope (Nikon). Scanning electron microscopy (SEM) was performed using a FEI Nova SEM 450 at an accelerating voltage of 5 kV at 1,000× magnification.

2.5 Gas Sensor Setup

The analyte gas NH_3 or HCl (0.05 %, 0.2%, N_2 fill) was diluted with nitrogen gas using a gas-mixing system, which consisted of two PTFE tubes from two flow-controllers (one from the NH_3 cylinder and one from the N_2 line) connecting via a Swagelok T-joint. The mixed gas was then passed through an additional gas mixing segment that constricts air-flow comprising of two mirroring tapered glass-needles, inserted into a short piece of PTFE tubing for support, to create gas turbulence and ensure adequate mixing. The relative flow rates of the two flow meters were then used to calculate the ppm concentrations of NH_3 or HCl being introduced into the cell.

3. Results and Discussion

3.1 Characterization of Au Microchannels and IL Microchannels

Physical characterization of the fabricated IL microchannels patterned onto a Au electrode are presented in Figure 1. Figure 1a shows the whole assembly of IL-based microchannels electrode which consisted of a micropatterned Au macrodisk working electrode, a Ag wire reference and a Pt wire counter electrode. A drop of IL ($[C_2mim][NTf_2]$ or $[C_4mpyrr][NTf_2]$) was drop-casted on the Teflon part of the working electrode which then connects the IL microchannels to the reference and counter electrodes The inset graph shows a zoomed-in image of the modified gold electrode surface with line micropatterns under a light microscope..
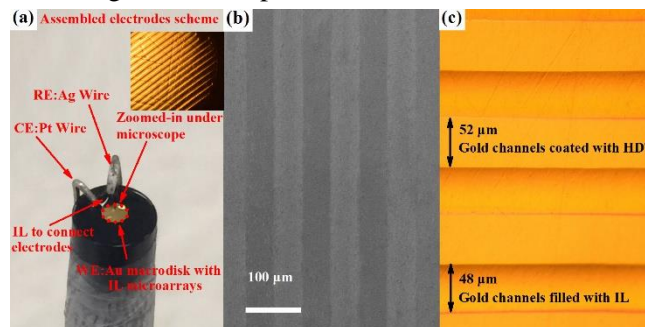

Figure 1. (a) Photo of the assembled IL-based microchannels electrode (b) Scanning electron microscopy (SEM) image of Au microchannels made by a HDT stamp on a gold substrate, and (c) Reflection microscopy image of the same Au microchannels (rotated by 90 degrees) filled with IL (width of Au microchannels is 48 μm and width of HDT microchannels is 52 μm).

Figure 1b shows the scanning electron microscopy (SEM) image for the Au microchannels (light grey color) and HDT microchannels (dark grey color) on the Au substrate. The HDT layer and bare Au microchannels are both presented with a spacing of 52 and 48 μm, respectively. Figure 1c shows the IL microchannels image taken by a reflection microscope showing clear straight edge on the IL microchannels. It can be seen that the IL selectively attaches to the Au microchannels, forming arrays of IL microbands with uniform shape and size. The darker shaded parts clearly show the edges of the microchannels occupied by RTILs. The height of the IL microchannels is approximately 9 μm, measured by scanning confocal microscopy. This gives an approximate total volume of 8.5 nL for the electrolyte solution filling the channels. HDT acts as a blocking surface – this was confirmed by covering the whole surface with HDT, with no voltammetric feaures observed upon exposure to the toxic gases.

3.2 Hydrogen Chloride Sensing

The electrochemical behaviour of the gas of interest was first studied in the two ionic liquids on the IL-microchannels electrode. Figure 2a shows the electrochemical oxidation of 500 ppm HCl gas on a $[C_2mim][NTf_2]$ microchannel-modified Au electrode. A clear oxidation peak corresponding to the two-electron oxidation of $[HCl_2]^-$ is observed on the Au surface. The mechanism for the hydrogen chloride reactions in ILs on Pt electrodes has been well studied and reported previously [19, 28, 29]. Since the numbers and approximate potentials of the peaks are similar, it is assumed that the reaction mechanism is similar on the gold surface. Hydrogen chloride dissolved in the IL is presented in the form of hydrogen dichloride ($[HCl_2]^-$) which is stable and discrete in ILs [30, 31]. The voltammetry on Au mainly shows the $[HCl_2]^-$ oxidation peak (I), followed by two reduction peaks, (II) and (III). The pre-peak before peak I in $[C_2mim][NTf_2]$ (Fig. 2a) could be related to water impurities in the RTIL, which are more obvious on gold surfaces due to gold oxide formation – similar behaviour was noted on gold screen-printed electrodes with RTILs, where additional voltammetric peaks were observed [35].
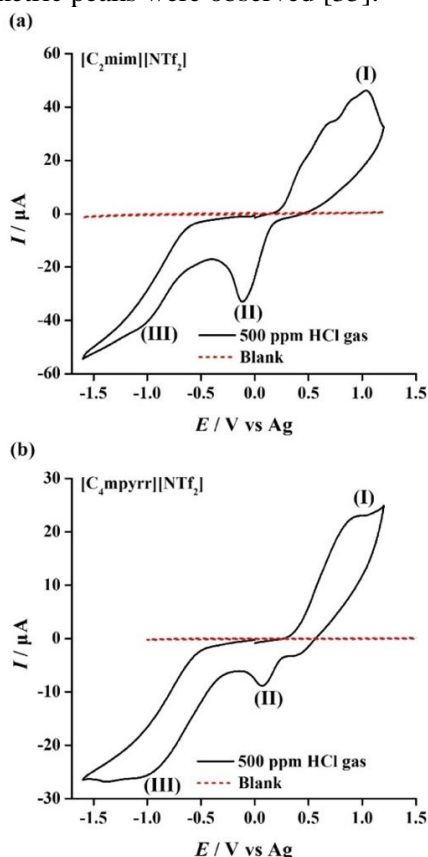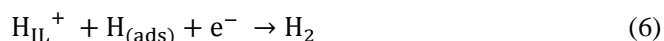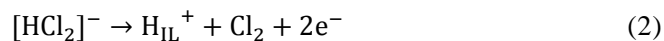
Those reactions have been investigated in detail by different groups [28, 29] and presented as the following equations (1 to 6):

$$H_{IL}^+ + 2Cl^- \rightarrow [HCl_2]^- \tag{1}$$

$$[HCl_2]^- \rightarrow H_{IL}^+ + Cl_2 + 2e^- \tag{2}$$

$$Cl_2 + e^- \rightarrow 2Cl^- \tag{3}$$

$$H_{IL}^+ + e^- \rightarrow H_{(ads)} \tag{4}$$

$$2H_{(ads)} \rightarrow H_2 \tag{5}$$

$$H_{IL}^+ + H_{(ads)} + e^- \rightarrow H_2 \tag{6}$$

Two reduction peaks were observed on the reverse sweep, corresponding to the reduction of two electrogenerated products: chlorine (eqn. 3, peak (II)) and solvated protons (eqn. 4, peak (III)). Silvester's group have reported that the solvated protons will be present once HCl is dissolved in the ILs [29]. The voltammetry obtained from another IL $[C_4mpyrr][NTf_2]$ (Figure 2b) is similar, and thus indicating that the electrochemical behaviour of hydrogen dichloride in ILs is mainly affected by the IL anion [19].

Figure 2. Cyclic voltammetry (CV) for the oxidation of 500 ppm hydrogen chloride gas on the (a) $[C_2mim][NTf_2]$ and (b) $[C_4mpyrr][NTf_2]$ microchannels-modified Au electrode at a scan rate of 100 mV s^{-1}. The dotted line is the response in the absence of hydrogen chloride gas.
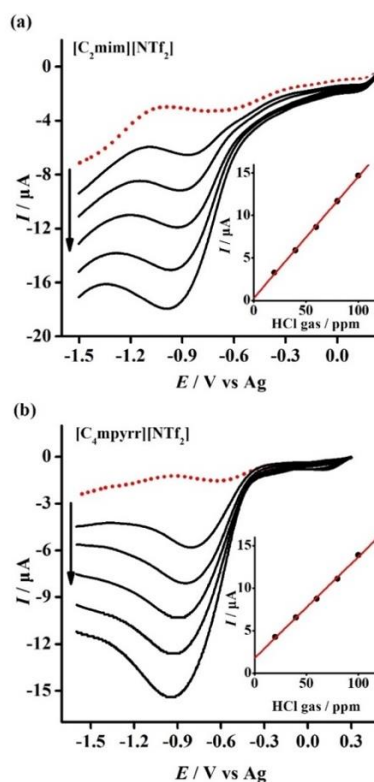

Figure 3. Linear sweep voltammetry (LSV) and corresponding calibration curves for the proton reduction peak at different concentrations of hydrogen chloride gas (0–100 ppm) on the (a) $[C_2mim][NTf_2]$ and (b) $[C_4mpyrr][NTf_2]$ microchannel-modified Au electrode at a scan rate of 100 mV s^{-1}. The dotted line is the response in the absence of hydrogen chloride gas.

The analytical response for current vs. concentration was studied on the $[C_2mim][NTf_2]$ and $[C_4mpyrr][NTf_2]$ microchannels-modified Au electrode in a relatively low concentration range of HCl gas from 20–100 ppm employing linear sweep voltammetry (LSV) as the detection technique. Instead of studying the oxidation peak, the proton reduction peak was selected as the best analytical signal since the oxidation peak is complicated (particularly on the gold surface) and lower LODs can be acquired using this peak, as previously reported by Murugappan *et al.* [19]. In addition, it enables the sensing of HCl in the presence of other interfering gases that can be oxidized (e.g. ammonia). The ability to choose the sensing peak is quite unique to the case of HCl (where HCl_2^- and H^+ is formed from two HCl molecules). Oxygen gas may be a possible interference due to its similar reduction potential in ILs, but this, and other gases that reduce can potentially be excluded by biasing at different potentials. However, as with all commercial sensors, it is difficult to eliminate all interferences.

Figure 3 shows LSV for the proton reduction peak (ca. -1.0 V vs Ag wire, peak III) of HCl gas at six different concentrations (0, 20, 40, 60, 80, 100 ppm) on the $[C_2mim][NTf_2]$ and $[C_4mpyrr][NTf_2]$ microchannels-modified Au electrode at a scan rate of 100 mV s^{-1}. The peak current (background subtracted) was plotted against the respective concentration to obtain calibration curves, as presented in the insets to Figure 3. As the concentration of HCl increases, the corresponding reduction peak current increases giving an excellent linearity ($R^2 > 0.99$) for the concentration range studied. Sensitivities are calculated from the gradient of the line of best fit while the LODs were calculated using three times the standard deviation of

the slope of the calibration line. LODs of 3.6 ppm and 5.2 ppm, and sensitivities of 1.43×10^{-7} A/ppm and 1.19×10^{-7} A/ppm, were obtained for $[C_2mim][NTf_2]$ and $[C_4mpyrr][NTf_2]$, respectively. The lowest LOD obtained from the $[C_2mim][NTf_2]$ microchannel electrode is lower than OSHA PEL for HCl (5 ppm) [24], suggesting that the sensor is suitable for the electrochemical detection of low concentrations of HCl.

In order to test the performance of the sensor for "real-time" HCl detection, chronoamperometry (CA) experiments were performed on the $[C_2mim][NTf_2]$ and $[C_4mpyrr][NTf_2]$ microchannels-modified Au electrode, as shown in Figure 4. First, a potential of -1.0 V vs. Ag was applied to the electrode and the system was purged with N_2 for sufficient time to obtain a stable baseline. HCl gas was introduced into the cell at different concentrations for 3 mins, while a N_2 "flushing" step was performed between each concentration change to ensure that the baseline is relatively stable. As shown in Figure 4, a relatively stable baseline current is observed in the absence of HCl at the beginning of the experiment. On the introduction of HCl gas, the current starts increasing and reaches a steady-state plateau. The sensors in this study not only give a stable current response but also present good reproducibility on different freshly prepared electrodes with only small (< 10 %) current variations. Furthermore, there is excellent repeatability (< 3 % current variation) on the same electrode for multiple additions of one chosen concentration of gas. The LODs obtained in $[C_2mim][NTf_2]$ and $[C_4mpyrr][NTf_2]$ are 4.8 ppm and 6.6 ppm, respectively. Compared with the results obtained from LSV, both LODs in these two ILs are slightly increased (3.6 ppm to 4.8 ppm and 5.2 ppm to 6.6 ppm).

Table 1. Analytical parameters from IL-based amperometric NH_3 and HCl sensors reported from the literature

Analyte	Working electrode	IL	Technique	LOD	Sensitivity	Response time	Reference
HCl	Pt SPE	$[C_2mim][NTf_2]$	LSV	3.4 ppm	29 nA/ppm	---	[22]
HCl	Pt μ-disk electrode	$[C_2mim][NTf_2]$	CV	69 ppm	1.75 pA/ppm	---	[19]
HCl	Au microchannels array	$[C_2mim][NTf_2]$	LSV	3.6 ppm	143 nA/ppm	---	This study
			CA	4.8 ppm	25.5 nA/ppm	t_{90}: 15-30s	
		$[C_4mpyr][NTf_2]$	LSV	5.2 ppm	119 nA/ppm	---	
			CA	6.6 ppm	21 nA/ppm	60-80s	
NH_3	Au microchannels array	$[C_2mim][NTf_2]$	LSV	4.1 ppm	14.4 nA/ppm	---	This study
			CA	6.2 ppm	1.8 nA/ppm	t_{90}: 15-30s	
		$[C_4mpyr][NTf_2]$	LSV	3.7 ppm	5.84 nA/ppm	---	
			CA	6.8 ppm	0.68 nA/ppm	15-30s	
NH_3	Pt SPE	$[C_2mim][NTf_2]$	LSV, CA	50 ppm	---	Several 100s	[35]
	Au SPE		LSV	185 ppm	---		
NH_3	HSA Pt/Au	$[C_4mim][NTf_2]$	CA	2 ppm	6.3 nA/ppm	t_{90}: 178s	[24]
NH_3	Pt SPE	$[C_2mim][TFB]$	CA	0.27 ppm	3.54 nA/ppm	t_{10-90}: 140s	[23]
		$[C_4mpyr][DCN]$	CA	0.12 ppm	2.63 nA/ppm	200s	
		$[C_4mpyr][NTf_2]$	CA	0.47 ppm	0.39 nA/ppm	370s	

NH$_3$	Pt TFE	[C$_2$mim] [NTf$_2$] LSV	2.7 ppm	1.1 nA/ppm	---	[20]
	Pt SPE		9.2 ppm	16 nA/ppm	---	
	Pt μ-disk electrode		2.7 ppm	1.5 pA/ppm	---	
	Pt MATFE (filled)		0.02 ppm	40 pA/ppm	---	
	Pt MATFE (Recessed)		0.11 ppm	49 pA/ppm	---	
NH$_3$	Pt MATFE	[C$_2$mim] [NTf$_2$] LSV	2.0 ppm	40.4 pA/ppm	---	[41]

Abbreviations: HSA= high surface area, SPE=screen-printed electrode, TFE= thin film electrode, MATFE= microarray thin-film electrode, CV-cyclic voltammetry, LSV=linear sweep voltammetry, CA=chronoamperometry
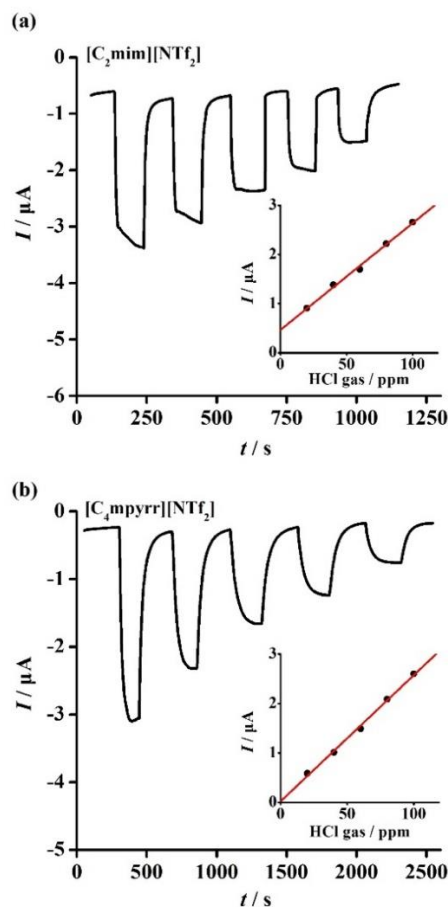
Figure 4. Chronoamperometry (CA) and the corresponding calibration curve for 0–100 ppm HCl gas on the (a) [C$_2$mim][NTf$_2$] and (b) [C$_4$mpyrr][NTf$_2$] microchannels-modified Au electrode holding the potential at −1.0 V vs. Ag.

The response times (τ_{90}) obtained in [C$_2$mim][NTf$_2$] (15–30 s) and [C$_4$mpyrr][NTf$_2$] (60–80 s) are much faster than that reported for commercial HCl AGS (Alphasense HCl-A1 series, 100–250 s) [32]. They are also faster than that observed on a Au macrodisk electrode in the absence of the channels (e.g. ~280 s for 60 ppm HCl, using 2 μL [C$_2$mim][NTf$_2$], results not shown here). These results confirm that the fast response time can be attributed to the presence of the microchannel structures and the small volumes of solvent required. Compared to other groups' work (Table 1), the IL-based microchannels HCl sensor developed in this study showed superior performance in response time, sensitivity and LOD. Interestingly, sensors based on [C$_4$mpyrr][NTf$_2$] show slightly higher sensitivity than [C$_2$mim][NTf$_2$] using CA (2.55×10^{-8} A/ppm vs. 2.10×10^{-8} A/ppm). However, the, least viscous [C$_2$mim][NTf$_2$] is preferred for long term analyte detection due to its faster τ_{90}, excellent linearity ($R^2 =0.998$) and lower LOD (below the 5 ppm OSHA PEL for HCl). The LODs obtained by CA are lower than the range of Emergency Exposure Guidance Level (EEGL, 10 min for 100 ppm and 20 ppm for 24 h) [33, 34]. The [C$_4$mpyrr][NTf$_2$]-based microchannels sensor with the CA technique is easily able to detect low enough concentrations for a toxic gas leak since the Immediately Dangerous to Life or Health (IDLH) concentrations are above 50 ppm.
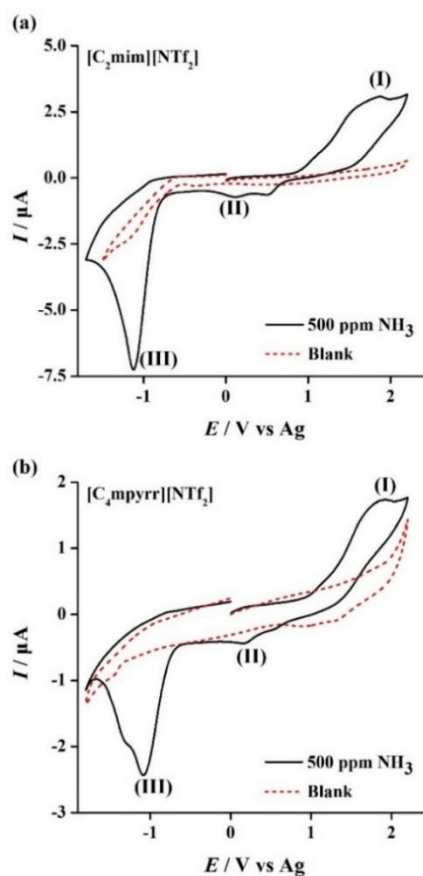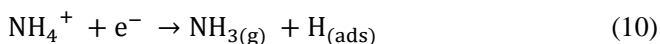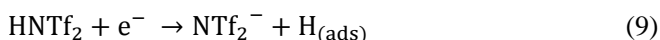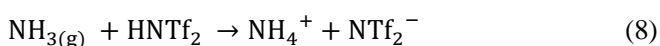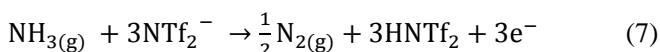
3.3 Ammonia Sensing

Figure 5. Cyclic voltammetry (CV) for the oxidation of 500 ppm ammonia gas on the (a) $[C_2mim][NTf_2]$ and (b) $[C_4mpyrr][NTf_2]$ microchannels-modified Au electrode at a scan rate of 100 mV s^{-1}. The dotted line is the response in the absence of ammonia.

Figure 5a shows the CV of 500 ppm NH_3 gas on a $[C_2mim][NTf_2]$ microchannels-modified Au electrode with a scan rate of 100 mV s^{-1}. Clear oxidation and reduction peaks for NH_3 (500 ppm) are observed on the Au surface while there is a relatively flat line obtained on the blank scan in the absence of ammonia. The mechanism for the oxidation of ammonia on different electrodes (Pt/Au/GC macrodisk and Pt microelectrode) has been reported previously [35-37]. The voltammetry mainly shows the ammonia oxidation peak (I), followed by several reduction peaks (II) and (III). These peaks are similar to the reported results on a Pt microelectrode [38] corresponding to the following reactions (Eqn. 7 to 10):

$$NH_{3(g)} + 3NTf_2^- \rightarrow \frac{1}{2}N_{2(g)} + 3HNTf_2 + 3e^- \qquad (7)$$

$$NH_{3(g)} + HNTf_2 \rightarrow NH_4^+ + NTf_2^- \qquad (8)$$

$$HNTf_2 + e^- \rightarrow NTf_2^- + H_{(ads)} \qquad (9)$$

$$NH_4^+ + e^- \rightarrow NH_{3(g)} + H_{(ads)} \qquad (10)$$

Briefly, NH_3 is oxidized (at ca. 1.9 V vs Ag wire) and a solvated proton (e.g. $HNTf_2$) is generated which then transferred to another NH_3 molecule in a chemical step as shown in eqn. 8. On the reverse sweep, there are two main reduction processes (eqn. 9 reduction of $HNTf_2$ and eqn. 10 reduction of NH_4^+). The voltammetry obtained from $[C_4mpyrr][NTf_2]$ (Figure 5b) is similar, indicating that NH_3 gas behaviour in ILs is less affected by the cation [36].

Figure 6 shows LSV for the oxidation of NH_3 gas at six different concentrations (0, 20, 40, 60, 80, 100 ppm) on the $[C_2mim][NTf_2]$ and $[C_4mpyrr][NTf_2]$ microchannels-modified Au electrode at a scan rate of 100 mV s^{-1}. The peak current (background subtracted) was plotted against the respective concentrations to obtain calibration curves, shown as the insets in figure 6. As the concentration of NH_3 goes up the corresponding oxidation peak current increases as well and an excellent linearity ($R^2 > 0.99$) was obtained for the concentration range studied. LODs of 4.1 ppm and 3.7 ppm, and sensitivities of 1.44×10^{-8} A/ppm and 5.84×10^{-9} A/ppm, were obtained for $[C_2mim][NTf_2]$ and $[C_4mpyrr][NTf_2]$, respectively. The LODs obtained are much lower than the previous reports on a gold screen-printed electrode (185 ppm), and the Occupational Safety and Health Administration Permissible Exposure Limit (OSHA PEL) for NH_3 (25

ppm) [35]. These results suggest that the two IL-based microchannels sensors are suitable for the electrochemical detection of low concentrations of NH_3. The higher sensitivity obtained from $[C_2mim][NTf_2]$ also reveals that the less viscous IL (viscosity of $[C_2mim][NTf_2]$ 34 cP [39] vs. $[C_4mpyrr][NTf_2]$ 79 cP [40]) is favoured for better NH_3 sensing performance.

CA for the oxidation of NH_3 was performed on the $[C_2mim][NTf_2]$ and $[C_4mpyrr][NTf_2]$ microchannels-modified Au electrodes and is shown in Figure 7. The potential was fixed at +1.8 V vs. Ag. When NH_3 gas is introduced into the system, the current starts to increase and reaches a plateau. Compared to $[C_2mim][NTf_2]$, it is harder to reach a plateau within a limited time in $[C_4mpyrr][NTf_2]$, likely due to its higher viscosity.
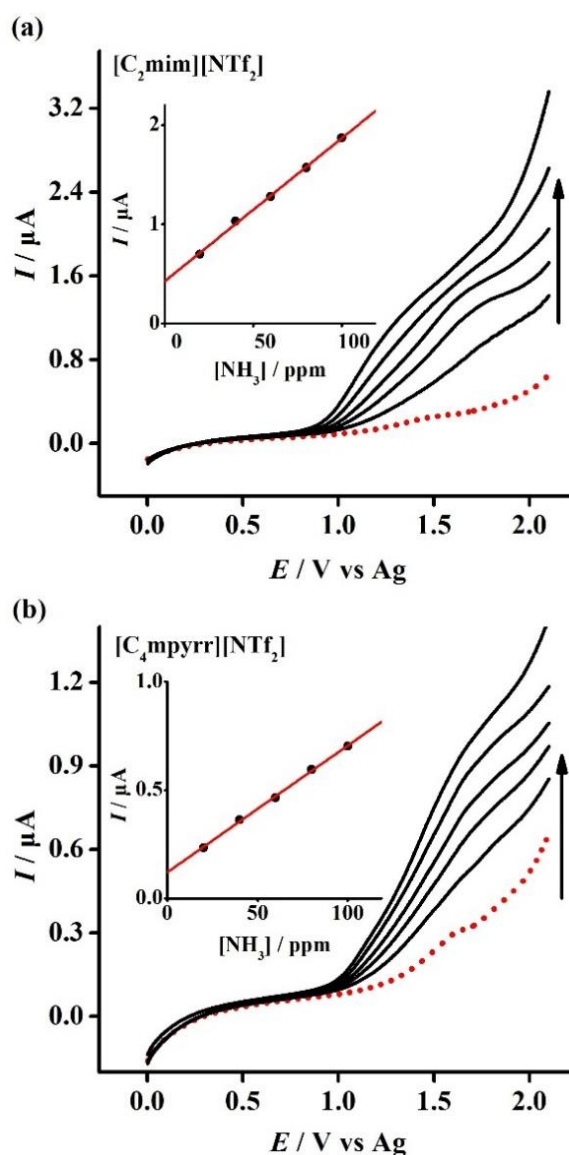

Figure 6. Linear sweep voltammetry (LSV) and corresponding calibration curves for the oxidation of ammonia (0-100 ppm) on the (a) $[C_2mim][NTf_2]$ and (b) $[C_4mpyrr][NTf_2]$ microchannels-

modified Au electrode at a scan rate of 100 mV s^{-1}. The dotted line is the response in the absence of ammonia.

LODs of 6.2 ppm and 6.8 ppm, and sensitivities of 1.80×10^{-9} A/ppm and 6.84×10^{-10} A/ppm were obtained by CA in [C$_2$mim][NTf$_2$] and [C$_4$mpyrr][NTf$_2$], respectively. Compared with other IL-based gas sensors reported before (τ_{90} of several 100 s) [35], the τ_{90} obtained in both RTILs microchannels sensor is 15-30 s, demonstrating the superior response time of our sensor design.
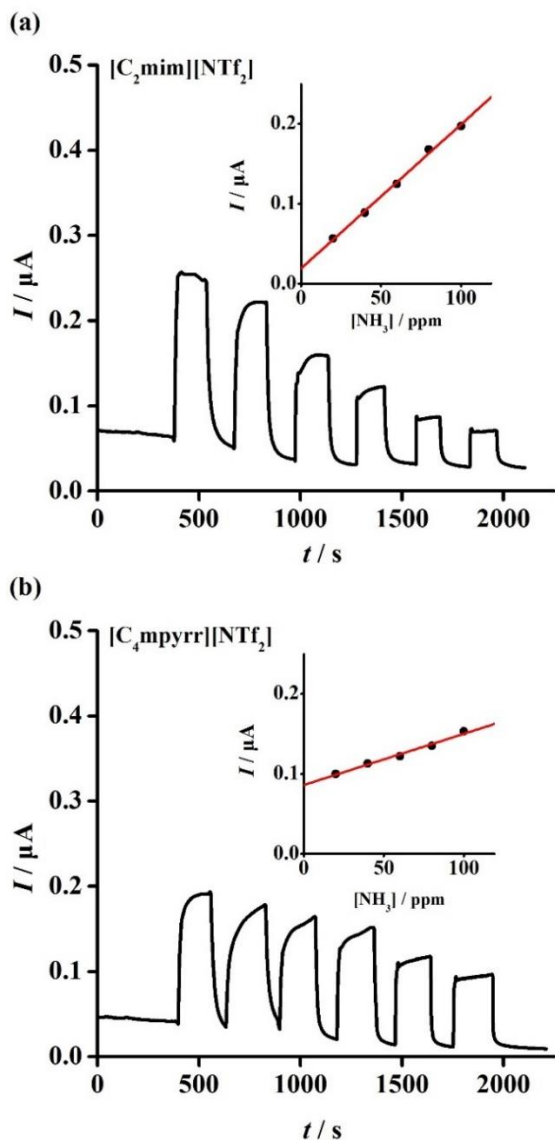
(a)

(b)

Figure 7. Chronoamperometry (CA) and corresponding calibration curve for 0–100 ppm ammonia on the (a) [C$_2$mim][NTf$_2$] and (b) [C$_4$mpyrr][NTf$_2$] microchannels-modified Au electrode holding the potential at +1.8 V vs. Ag.

Observations from the above results indicate that real-time measurement of NH$_3$ concentration is highly accessible by using CA with this sensor design. Compared with the results obtained by LSV, it is suggested that the LSV technique is more suitable and sensitive for lower concentrations of NH$_3$ sensing with a higher sensitivity and a lower LODs. Similar behavior was reported by Hussain *et al.* who studied voltammetric techniques comparison for NH$_3$ sensing in [C$_2$mim][NTf$_2$] [41]. They pointed out that the LSV technique presents the best sensitivity among LSV, DPV (differential pulse voltammetry) and SWV (square wave voltammetry) for NH$_3$ sensing. It is worth noting that both calibration curves with background subtraction in CA and LSV do not pass directly through the origin. However, it is not unusual to observe such behaviour for gas sensing in RTILs due to various factors such as an unstable background current , shifting of the reference potential or electrical noise. Even for a commercialised gas sensor (from KWJ Engineering Inc) a calibration curve showed a positive y-intercept for ammonia detection [42]. However, overall, the analytical parameters (low LOD, high sensitivity and fast response time) presented in table 1 show a promising prospect of IL-based microchannel array sensors for toxic gas detection.

4. Conclusion

An IL-based microchannel array sensor design has been developed for the sensitive and fast detection of the toxic gases NH$_3$ and HCl. The electrochemical behaviour of NH$_3$ and HCl was investigated in two different ILs ([C$_2$mim][NTf$_2$] and [C$_4$mpyrr][NTf$_2$]). The mechanism of both gases on the Au modified microchannels electrode was very similar to the reported behaviour on conventional Pt/Au microelectrodes or screen printed electrodes. It is suggested that HDT (which is used to block the specific area of the gold surface to form microchannels) is inactive to the toxic gases. On the timescale of the electrochemical experiments, no unusual behaviour or detrimental effects were observed on the Au modified microchannels electrode. Very low LODs were obtained from [C$_2$mim][NTf$_2$] and [C$_4$mpyrr][NTf$_2$] via LSV (4.1 ppm and 3.7 ppm for NH$_3$, 3.6 ppm and 5.2 ppm for HCl). The obtained analytical parameters suggest that the proposed sensor design has a far superior performance both in sensitivity and response time compared to the commercially available and reported sensors to date. This IL-based microchannel sensor shows a promising prospective for the detection of a range of highly toxic gases with enhanced

sensitivity and response times for real-time environmental monitoring.

Acknowledgements

References

[1] R.A. Alvarez, S.W. Pacala, J.J. Winebrake, W.L. Chameides, S.P. Hamburg, *Proc. Natl. Acad. Sci. U.S.A.* **2012**, *109*, 6435-6440.

[2] E. Krausmann, A.M. Cruz, B. Affeltranger, *J. Loss Prev. Process Ind.* **2010**, *23*, 242-248.

[3] K. McKain, A. Down, S.M. Raciti, J. Budney, L.R. Hutyra, C. Floerchinger, S.C. Herndon, T. Nehrkorn, M.S. Zahniser, R.B. Jackson, *Proc. Natl. Acad. Sci. U.S.A.* **2015**, *112*, 1941-1946.

[4] S.M. Roe, M.D. Spivey, H.C. Lindquist, K.B. Thesing, R.P. Strait, *Estimating ammonia emissions from anthropogenic nonagricultural sources – Draft final report* **2004**.

[5] W.B. Faulkner, B.W. Shaw, *Atmos Environ* **2008**, *42*, 6567-6574.

[6] R. Verma, K. Vinoda, M. Papireddy, A. Gowda, *Procedia Environ Sci* **2016**, *35*, 701-708.

[7] M.W.M. Hisham, T.V. Bommaraju, *Hydrogen chloride in ECT(online) 5th ed, Kirk-Othmer Encyclopedia of Chemical Technology Vol. 13*, **2000**, pp. 803-837.

[8] P. Colonna, S. Gabrielli, *Appl. Therm. Eng.* **2003**, *23*, 381-396.

[9] D.E. Malek, Y. Alarie, *Toxicol. Appl. Pharmacol.* **1989**, *101*, 340-355.

[10] R.B. Swotinsky, K.H. Chase, *Am. J. Ind. Med.* **1990**, *17*, 515-521.

[11] M.H. Hammond, K.J. Johnson, S.L. Rose-Pehrsson, J. Ziegler, H. Walker, K. Caudy, D. Gary, D. Tillett, *Sens Actuators B Chem* **2006**, *116*, 135-144.

[12] L. Barrosse‐Antle, A. Bond, R. Compton, A. O'Mahony, E. Rogers, D. Silvester, *Chem Asian J* **2010**, *5*, 202-230.

[13] D.S. Silvester, R.G. Compton, *Z. Phys. Chem.* **2006**, *220*, 1247-1274.

[14] L. Xiong, R.G. Compton, *Int. J. Electrochem. Sci* **2014**, *9*, 7152-7181.

[15] A. Yokozeki, M.B. Shiflett, *Ind. Eng. Chem. Res.* **2007**, 46, 1605-1610.

[16] Z. Lei, C. Dai, B. Chen, *Chem. Rev.* **2014**, *114*, 1289-1326.

[17] H. Liu, S. Dai, D.-e. Jiang, *J. Phys. Chem. B* **2014**, *118*, 2719-2725.

[18] B.R. Prasad, S. Senapati, *J. Phys. Chem. B* **2009**, *113*, 4739-4743.

[19] K. Murugappan, D.S. Silvester, *Phys. Chem. Chem. Phys.* **2016**, *18*, 2488-2494.

[20] G. Hussain, D.S. Silvester, *Anal. Chem.* **2016**, *88*, 12453-12460.

[21] K. Crowley, E. O'Malley, A. Morrin, M.R. Smyth, A.J. Killard, *Analyst* **2008**, *133*, 391-399.

[22] K. Murugappan, D.W. Arrigan, D.S. Silvester, *J. Phys. Chem. C* **2015**, *119*, 23572-23579.

[23] M.T. Carter, J.R. Stetter, M.W. Findlay, V. Patel, *ECS Trans.* **2014**, *64*, 95-103.

[24] M.T. Carter, J.R. Stetter, M.W. Findlay, V. Patel, *ECS Transactions* **2012**, *50*, 211-220.

[25] C.A. Gunawan, M.C. Ge, C. Zhao, *Nat. Commun.* **2014**, *5*, 3744.

[26] R. Gondosiswanto, C.A. Gunawan, D.B. Hibbert, J.B. Harper, C. Zhao, *ACS Appl. Mater. Interfaces* **2016**, *8*, 31368-31374.

[27] D. Qin, Y. Xia, G.M. Whitesides, *Nat. Protoc.* **2010**, 5, 491.

[28] L. Aldous, D.S. Silvester, W.R. Pitner, R.G. Compton, M.C. Lagunas, C. Hardacre, *J. Phys. Chem. C* **2007**, *111*, 8496-8503.

[29] K. Murugappan, D.S. Silvester, *Sensors* **2015**, *10*, 26866-26876.

[30] P.J. Dyson, M.C. Grossel, N. Srinivasan, T. Vine, T. Welton, D.J. Williams, A.J. White, T. Zigras, *J. Chem. Soc., Dalton Trans.* **1997**, *19*, 3465-3469.

[31] J.L. Campbell, K.E. Johnson, J.R. Torkelson, *Inorg. Chem.* **1994**, *33*, 3340-3345.

[32] T.J. Roberts, T. Lurton, G. Giudice, M. Liuzzo, A. Aiuppa, M. Coltelli, D. Vignelles, G. Salerno, B. Couté, M. Chartier, R. Baron, J.R. Saffell, B. Scaillet, *Bull. Volcanol.* **2017**, *79*, 36.

[33] R.P. Pohanish, *Sittig's handbook of toxic and hazardous chemicals and carcinogens* **2017**.

[34] C.G. Association, *Handbook of compressed gases* **1999**.

[35] K. Murugappan, J. Lee, D.S. Silvester, *Electrochem. Commun.* **2011**, *13*, 1435-1438.

[36] X. Ji, C.E. Banks, D.S. Silvester, L. Aldous, C. Hardacre, R.G. Compton, *Electroanalysis* **2007**, *19*, 2194-2201.

[37] M.C. Buzzeo, D. Giovanelli, N.S. Lawrence, C. Hardacre, K.R. Seddon, R.G. Compton, Electroanalysis **2004**, 16, 888-896.

[38] X. Ji, D.S. Silvester, L. Aldous, C. Hardacre, R.G. Compton, *J. Phys. Chem. C* **2007**, *111*, 9562-9572.

[39] P. Bonhote, A.-P. Dias, N. Papageorgiou, K. Kalyanasundaram, M. Grätzel, *Inorg. Chem.* **1996**, *35*, 1168-1178.

[40] C. Xiao, A. Rehman, X. Zeng, *Anal. Chem.* **2012**, *84*, 1416-1424.

[41] G. Hussain, D.S. Silvester, *Electroanalysis* **2018**, *30*, 75-83.

[42] M.T. Carter, J.R. Stetter, M.W. Findlay, V. Patel, ECS Transactions 2014, 58, 7-18.